



Published in final edited form as:

Cell Rep. 2021 August 24; 36(8): 109584. doi:10.1016/j.celrep.2021.109584.

The macrophage-derived protein PTMA induces filamentation of the human fungal pathogen *Candida albicans*

Nicola T. Case¹, Kwamaa Duah¹, Brett Larsen², Cassandra J. Wong², Anne-Claude Gingras^{1,2}, Teresa R. O'Meara³, Nicole Robbins¹, Amanda O. Veri¹, Luke Whitesell¹, Leah E. Cowen^{1,4,*}

¹Department of Molecular Genetics, University of Toronto, Toronto, ON M5S 1A8, Canada

²Lunenfeld-Tanenbaum Research Institute, Sinai Health System, Toronto, ON M5G 1X5, Canada

³Department of Microbiology and Immunology, University of Michigan, Ann Arbor, MI 48109, USA

⁴Lead contact

SUMMARY

Evasion of killing by immune cells is crucial for fungal survival in the host. For the human fungal pathogen *Candida albicans*, internalization by macrophages induces a transition from yeast to filaments that promotes macrophage death and fungal escape. Nutrient deprivation, alkaline pH, and oxidative stress have been implicated as triggers of intraphagosomal filamentation; however, the impact of other host-derived factors remained unknown. Here, we show that lysates prepared from macrophage-like cell lines and primary macrophages robustly induce *C. albicans* filamentation. Enzymatic treatment of lysate implicates a phosphorylated protein, and bioactivity-guided fractionation coupled to mass spectrometry identifies the immunomodulatory phosphoprotein PTMA as a candidate trigger of *C. albicans* filamentation. Immunoneutralization of PTMA within lysate abolishes its activity, strongly supporting PTMA as a filament-inducing component of macrophage lysate. Adding to the known repertoire of physical factors, this work implicates a host protein in the induction of *C. albicans* filamentation within immune cells.

Graphical Abstract

This is an open access article under the CC BY-NC-ND license (<http://creativecommons.org/licenses/by-nc-nd/4.0/>).

*Correspondence: leah.cowen@utoronto.ca.

AUTHOR CONTRIBUTIONS

N.T.C., N.R., A.O.V., L.W., and L.E.C. wrote the paper. N.T.C., K.D., B.L., C.J.W., A.-C.G., T.R.O., N.R., A.O.V., L.W., and L.E.C. designed the experiments and interpreted the data. N.T.C., K.D., B.L., and C.J.W. performed the experiments. L.E.C. and A.-C.G. provided the materials.

DECLARATION OF INTERESTS

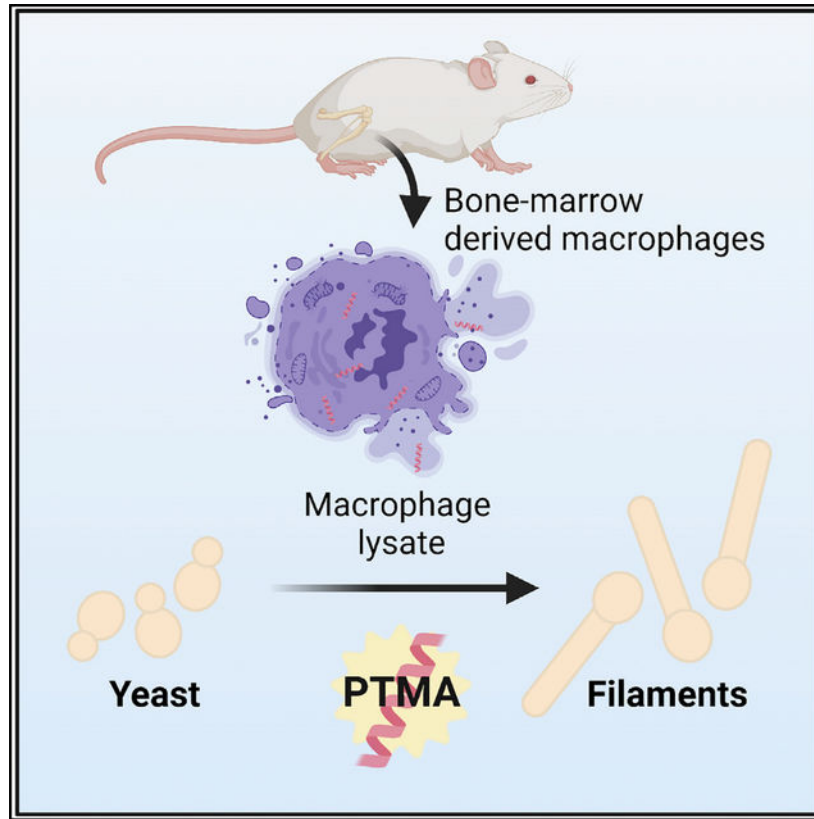
L.E.C. and L.W. are co-founders of and shareholders in Bright Angel Therapeutics, a platform company for development of novel antifungal therapeutics. L.E.C. is a consultant for Boragen, a small-molecule development company focused on leveraging the unique chemical properties of boron chemistry for crop protection and animal health.

INCLUSION AND DIVERSITY

One or more of the authors of this paper self-identifies as an underrepresented ethnic minority in science. One or more of the authors of this paper self-identifies as a member of the LGBTQ+ community. While citing references scientifically relevant for this work, we also actively worked to promote gender balance in our reference list.

SUPPLEMENTAL INFORMATION

Supplemental information can be found online at <https://doi.org/10.1016/j.celrep.2021.109584>.



In brief

The human fungal pathogen *Candida albicans* filaments within host macrophages, enabling its escape. Case et al. demonstrate that lysates prepared from macrophage-like cell lines and primary macrophages induce *C. albicans* filamentation and implicate the immunomodulatory protein prothymosin alpha (PTMA) as a trigger of filamentation produced by host immune cells.

INTRODUCTION

Fungi pose a serious threat to human health that is often underappreciated (Brown et al., 2012). While superficial fungal infections affect billions of people worldwide, systemic infections claim more than 1.5 million lives each year (Brown et al., 2012). *Candida albicans* is both a leading human fungal pathogen and a member of the human mucosal microbiota (Polvi et al., 2015). It is a common cause of superficial mucosal infections, such as oral thrush and vaginal yeast infections, but can also cause life-threatening systemic infections in immunocompromised individuals, with mortality rates upward of 40% (Brown et al., 2012). A major virulence trait of *C. albicans* is its ability to transition between yeast and filamentous morphologies. The yeast form of *C. albicans* is crucial for colonization and dissemination via the bloodstream, while the filamentous form enables tissue invasion and deep-seated infection (Saville et al., 2003). Accordingly, the ability of *C. albicans* to transition between yeast and filaments is strongly correlated with virulence, because

the majority of mutants locked in either state are avirulent in mouse models of systemic candidiasis (Lo et al., 1997; Murad et al., 2001; Noble et al., 2010; Saville et al., 2003).

Filamentation is regulated via complex genetic circuitry that enables *C. albicans* to respond to diverse stimuli within the host, including serum, elevated temperature, and 5% CO₂ (Sudbery, 2011). There are several core morphogenetic signaling cascades that are important for response to multiple cues, while others are more specialized (Shapiro et al., 2011). Ultimately, these cascades lead to the expression of hypha-specific genes and activation of cellular pathways that enable filamentous growth (Shapiro et al., 2011).

The morphological state adopted by *C. albicans* has major implications for its interactions with host immune cells (Netea et al., 2015). Macrophages readily engulf and internalize *C. albicans* yeast cells but are limited in their ability to phagocytose filaments because of their large size and shielding of inner cell wall components that trigger immune recognition (Erwig and Gow, 2016). Namely, although yeast cells expose the strong fungal recognition signal β -1,3-glucan at sites of bud scars, hyphae lack bud scars, leading to decreased recognition by macrophages via the C-type lectin receptor dectin-1 (Erwig and Gow, 2016). In addition to the role of morphogenesis in avoiding engulfment, once inside the macrophage phagosome, *C. albicans* undergoes filamentation coupled to cell wall remodeling that induces pyroptosis, a macrophage inflammatory cell death program, leading to fungal escape (O'Meara et al., 2015). Several physical factors in the macrophage phagosome have been implicated in triggering *C. albicans* filamentation, including, but not limited to, nutrient deprivation (Lorenz et al., 2004), alkaline pH (Vylkova and Lorenz, 2014, 2017), and oxidative stress (Shi et al., 2007). Although there are likely multiple factors that contribute to *C. albicans* intraphagosomal filamentation, a specific macrophage-derived factor that drives filamentation has yet to be discovered.

Here, we demonstrate that lysates derived from macrophage-like cell lines and primary macrophages are sufficient to induce *C. albicans* filamentation. Treatment of lysate with proteinase or phosphatase abolished its activity, indicating that a filament-inducing trigger within lysate is likely a phosphorylated protein. Additionally, bioactivity-guided fraction coupled to mass spectrometry (MS) identified the immunomodulatory protein, prothymosin alpha (PTMA), as the lead candidate. Immunoneutralization of PTMA within lysate abolished its ability to stimulate *C. albicans* filamentation, strongly supporting PTMA as a filament-inducing component of lysate derived from phagocytic cells. This work implicates a host-derived protein in the induction of *C. albicans* filamentation upon phagocytosis by macrophages and provides insights into the mechanisms underlying this complex host-pathogen interaction.

RESULTS

Macrophage lysate induces *C. albicans* filamentation

Phagocytosis by J774A.1 macrophage-like cells and bone marrow-derived macrophages (BMDMs) is well recognized to induce robust *C. albicans* filamentation (O'Meara et al., 2015, 2018; Figure 1A), yet insight into the macrophage-derived factors governing this response has remained elusive. To identify macrophage-derived triggers of *C. albicans*

filamentation, we prepared detergent-free whole-cell lysates from mouse (J774A.1 and RAW 264.7) and human (U937) cell lines of monocyte-macrophage lineage and tested their ability to induce filamentation. Although these cell lines consist of continuously proliferating cancer cells, they remain sufficiently differentiated to retain key functional characteristics of the mononuclear phagocyte system that plays a major role in the host immune response to invasive *C. albicans* infection and will be referred to as macrophage lines henceforth. We also prepared lysates from murine BMDMs in an analogous manner to assess the ability of lysate from primary macrophages to induce filamentation. To enable visualization and quantification of filamentation in subsequent assays, we used a *C. albicans* strain where GFP expression is driven by the filament-specific *HWPIp* promoter (*HWPIp*-GFP).

Incubation of *C. albicans* with lysates prepared from J774A.1, RAW 264.7, or U937 cells for 6 h at 30°C induced filamentation, as indicated by the cellular morphology and GFP expression (Figure 1B). We also found that incubation of *C. albicans* with lysate prepared from murine BMDMs induced robust filamentation (Figure 1C), indicating that the filament-inducing activity is preserved in primary macrophages. Notably, no filamentation was observed in *C. albicans* cells incubated with RPMI medium alone, the medium in which lysates were prepared (Figures 1B and 1C). To address the potential contribution to lysate activity of residual serum from the culture medium in which the phagocytic cells are grown, despite dilution of the culture medium by at least 100-fold during lysate preparation, we incubated the *HWPIp*-GFP strain in medium containing 10% serum for 6 h at 30°C. As expected, even 10% serum was insufficient to induce filamentation under these conditions, given the temperature requirement of at least 37°C for serum-induced filamentation (Shapiro and Cowen, 2012); these were the same conditions under which lysate induces filamentation, confirming that any residual serum present in lysate does not contribute to its activity (Figure S1A). To further characterize the filament-inducing activity of macrophage lysate, we focused on J774A.1 cells, a cell line amenable to large-scale lysate production and one that has been widely used to investigate *C. albicans*-macrophage interactions (Bain et al., 2014, 2021; Lorenz et al., 2004; O'Meara et al., 2015, 2018; Wartenberg et al., 2014). To quantify the degree of filamentation induced by varying concentrations of lysate, we analyzed the *HWPIp*-GFP strain by microscopy and flow cytometry (Figures 1D–1F). Consistent with microscopic observations, we saw a marked increase in the percentage of GFP⁺ cells with increasing concentrations of macrophage lysate, which saturated at a lysate total protein concentration of approximately 50 µg/mL (Figures 1D–1F). These results confirm that macrophage lysate induces *C. albicans* filamentation in a concentration-dependent manner.

Bioactivity-guided fractionation of macrophage lysate identifies filament-inducing protein candidates

To characterize the properties of the filament-inducing factor(s) within macrophage lysate, we treated lysate with Proteinase K and calf intestinal phosphatase (CIP). As expected, *C. albicans* *HWPIp*-GFP cells incubated with untreated or phosphatase-buffer-only-treated control lysates underwent robust filamentation; however, cells incubated with lysate pre-treated with either enzyme did not filament (Figure 2A). Consistent with these observations, cells incubated in lysate pre-treated with Proteinase K or CIP displayed a large decrease

in the percentage of GFP⁺ cells relative to cells incubated with control lysates when quantified by flow cytometry (Figures 2B and 2C). Notably, incubation of *HWPIp*-GFP cells with RPMI medium that had been pre-treated with Proteinase K or CIP did not block filamentation induced by an alternate cue, elevated temperature, demonstrating that the enzymes themselves do not block filamentation (Figure S1B). Together, these results suggest that a phosphorylated protein or peptide is likely responsible for the filament-inducing activity of macrophage lysate.

To identify macrophage-derived protein candidates responsible for inducing *C. albicans* filamentation, we analyzed macrophage lysate by bioactivity-guided fractionation coupled to MS. Lysate was fractionated by reverse-phase liquid chromatography via stepwise elution with increasing concentrations of acetonitrile (ACN), and after solvent removal, fractions were subsequently tested for their ability to induce filamentation of a standard laboratory *C. albicans* strain (SN95). Fractions were scored for their filament-inducing activity on a scale from 0 to 3, where 0 signifies yeast, 1 signifies short filaments or pseudohyphae, 2 signifies a mixed population of yeast and filaments, and 3 signifies predominantly filaments. Incubation of *C. albicans* with the fraction eluted with 25% or 35% ACN resulted in a population of cells that were predominantly filamentous (score of 3; Figure 2D). MS analysis of the fractions' peptide content demonstrated they were highly complex, with over 200 proteins detected with greater than 2 spectral counts in the fractions that induced the most robust levels of filamentation (25% and 35% ACN). Many proteins were detected in multiple fractions, but of the 25 proteins detected with the most spectral counts in the 35% ACN fraction, 23 were detected at higher amounts in this fraction than any other fraction. Of these proteins, our attention was drawn to the immunomodulatory protein, PTMA, for which the greatest number of spectral counts was detected in the 35% ACN fraction (Figure 2E). Although detected at lower levels in all fractions, including the 25% ACN fraction, the greatest number of spectra mapping to PTMA was detected in the 35% ACN fraction (Figure 2E; Table S1). Interestingly, four of the seven proteins with the greatest number of spectra in the 35% ACN fraction included the high-mobility group box proteins (HMGB1 and HMGB2) and histone proteins (HIST1H2BE and HIST2H2BB), which are recognized damage-associated molecular patterns (DAMPs; Roh and Sohn, 2018). Notably, PTMA has been proposed as a candidate DAMP (Samara et al., 2016).

PTMA is a phosphorylated protein present in mammals and teleosts with roles in promoting cell proliferation and mediating immunity (Samara et al., 2016). The full-length protein is cleaved by intracellular proteases into several bioactive peptides that display diverse cellular activities, some of which are being explored for therapeutic applications (Samara et al., 2016). MS analysis determined that the sequence coverage for PTMA in the 35% ACN fraction was 68% (Figure 2F). We detected peptides that mapped to two fragments of PTMA known to be generated endogenously (Samara et al., 2016), thymosin alpha 1 (residues 1–28) and the carboxy-terminal peptide (residues 100–111; Figure 2F; Table S2). Of the 295 spectra detected in the 35% ACN fraction for peptides mapping to PTMA, the majority mapped to the last 22 amino acids of the C terminus (Figure 2F). Interestingly, compared with the 35% ACN fraction, very few peptides mapped to the N terminus of PTMA in the fraction eluted with 25% ACN, where filamentation was also observed in the majority of cells (Figures 2D and S2).

PTMA is required for lysate-induced filamentation

We next sought to determine whether PTMA is sufficient to induce filamentation in *C. albicans* and/or necessary for macrophage lysate-induced filamentation. To test for sufficiency, we assayed recombinant PTMA purified from the model yeast *Saccharomyces cerevisiae* in a background concentration of lysate that does not induce filamentation to place the protein in a native environment and reduce non-specific adsorption to surfaces. Under conditions in which macrophage lysate induces filamentation in the *HWPIp*-GFP strain, we found that PTMA purified from *S. cerevisiae* was insufficient to trigger filamentation, perhaps because of factors such as the absence of native phosphorylation or processing (Figure S3).

We explored two approaches to investigate whether PTMA is required for the filament-inducing activity of macrophage lysate. First, we attempted RNAi-mediated knockdown of its expression in our macrophage cell line using an optimized microRNA system (Fellmann et al., 2013). Consistent with evidence for an essential role of PTMA in the growth and survival of diverse cell lines, especially those of hematopoietic origin (Cancer Dependency Map: <https://depmap.org/portal/gene/PTMA>; Tsherniak et al., 2017), we were unable to isolate any lineages demonstrating stable depletion of PTMA. Given that knockout of PTMA is embryonic lethal in mice (Dickinson et al., 2016) and is not tolerated in diverse hematopoietic cell lines (Tsherniak et al., 2017), we did not attempt to knock out PTMA in our macrophage line.

As an alternative to genetic depletion of PTMA, we adopted an immunoneutralization approach. We incubated J774A.1 macrophage lysate overnight at 4°C with antibodies against either the N or C terminus of PTMA and found that both reagents blocked lysate-induced filamentation (Figures 3A–3F). Incubation with a rabbit antiserum raised against an N-terminal PTMA epitope reduced the ability of lysate to induce filamentation in the *HWPIp*-GFP strain (Figure 3A) and resulted in a near-complete loss of GFP⁺ cells relative to non-immune rabbit serum as control (Figures 3B and 3C). The specificity of this neutralization activity for PTMA was confirmed by incubating lysate with an independent C-terminal-targeted anti-PTMA antibody raised in rabbit. This affinity-purified antibody abolished the ability of lysate to induce filamentation (Figure 3D) and again greatly decreased the percentage of GFP⁺ cells relative to polyclonal rabbit IgG as control (Figures 3E and 3F). Similarly, we found that treatment of lysate derived from murine BMDMs with the C-terminal anti-PTMA antibody blocked its filament-inducing activity (Figure 3G). Notably, incubation of the *HWPIp*-GFP strain with RPMI medium treated with either anti-PTMA antibody preparation did not block filamentation induced by elevated temperature, demonstrating that the antibodies themselves do not block filamentation (Figure S1C). Together, these results indicate that PTMA is required for the filament-inducing activity of macrophage lysate.

DISCUSSION

For the major human fungal pathogen *C. albicans*, filamentation upon internalization by host immune cells is a key virulence trait that promotes phagocyte death and fungal escape (O'Meara et al., 2015). Here, we show that PTMA is required for the ability of macrophage

lysate to induce *C. albicans* filamentation. However, the underlying mechanisms and broader implications of this activity in the context of the host remain to be elucidated. PTMA functions both intracellularly and extracellularly, where it acts to potentiate transcription (Karetsou et al., 2002), remodel chromatin (Gómez-Márquez and Rodríguez, 1998), inhibit apoptosis (Jiang et al., 2003), and stimulate cells of the innate and adaptive immune system (Baxevanis et al., 1990, 1992; Cordero et al., 1992; Heidecke et al., 1997). The full-length protein and its native proteolytic fragments possess a wide range of therapeutic effects, such as anticancer and antiviral activities, which have been recently reviewed (Samara et al., 2016). Interestingly, subcutaneous administration of the N-terminal peptide, thymosin alpha 1, to mice before intravenous challenge with *C. albicans* protected against lethal infection (Bistoni et al., 1982). Additionally, in a model of bone marrow transplantation, thymosin alpha 1 protected against invasive aspergillosis, and pre-exposure of alveolar macrophages and circulating neutrophils to thymosin alpha 1 *in vitro* was shown to potentiate their phagocytic and conidiocidal activity (Romani et al., 2004). This suggests that the protective effects of thymosin alpha 1 may be due in part to its ability to activate phagocytic cells (Romani et al., 2004). In considering whether PTMA might play an additional role at the host-pathogen interface by stimulating *C. albicans* filamentation within the macrophage phagosome, several questions warrant further investigation.

One crucial issue is if, when, and how PTMA localizes to the *C. albicans*-containing phagosome. Notably, PTMA localization is predominantly nuclear in most cells, but cytoplasmic localization is observed in the cells of the stomach (Kijogi et al., 2016), and during apoptosis is associated with caspase-3-mediated cleavage of the nuclear localization sequence (NLS) of PTMA (Evstafieva et al., 2003). However, to our knowledge, the subcellular localization of PTMA in macrophages has not been investigated under normal physiological conditions or during infection. Of all tissues examined, PTMA is most highly expressed in monocytes (Samaras et al., 2020; Schmidt et al., 2018), the progenitors of tissue macrophages. Thus, PTMA could be targeted to phagosomes during macrophage differentiation or upon the activation that accompanies engulfment of *C. albicans*. Indeed, PTMA may localize to the phagosome, as occurs with antimicrobial peptides such as LL-37 during *Mycobacterium tuberculosis* infection (Rivas-Santiago et al., 2008). Alternatively, PTMA may bind to *C. albicans* prior to ingestion by macrophages. Extracellular binding of PTMA to *C. albicans* could occur while *C. albicans* circulates in the blood, because PTMA is present at 620 ng/L in human plasma (Deutsch et al., 2005), or could occur locally in the tissue microenvironment prior to phagocytosis. Given its ubiquitous expression (Samara et al., 2016), PTMA may be present locally by passive release from dying cells or through active export by neighboring cells. Although PTMA lacks a signal peptide sequence, neurons release PTMA upon serum-deprivation stress in a manner that is dependent on the cargo protein S100A13 (Matsunaga and Ueda, 2010), suggesting a possible mechanism for non-vesicular release of PTMA from cells. Thus, there could be multiple non-mutually exclusive mechanisms by which PTMA and *C. albicans* may come to interact within the macrophage phagosome.

Another key question to address is the mechanism by which PTMA induces *C. albicans* filamentation. Perhaps PTMA binds to a receptor on the surface of *C. albicans* that transmits a signal to induce filamentation. Such signaling cascades are known to occur through

membrane-associated sensors that mediate filamentation in response to nitrogen starvation (Mep2), the amino acids proline and methionine (Gpr1), and alkaline pH (Rim21 and Dfg16; Shapiro et al., 2011). Alternatively, PTMA may partially insert into or transit the plasma membrane as shown for some antimicrobial peptides (Matejuk et al., 2010), such as histatin 5, a cell-penetrating antimicrobial peptide with candidacidal activity that targets the mitochondrion (Helmerhorst et al., 1999). Consistent with this hypothesis, the N terminus of PTMA inserts into and interacts with the negatively charged components of model membranes (Mandaliti et al., 2016; Nepravishita et al., 2015). If PTMA transits the fungal plasma membrane, perhaps it induces filamentation by modulating gene transcription in the nucleus. Indeed, PTMA potentiates transcription (Karetsov et al., 2002) and remodels chromatin (Gómez-Márquez and Rodríguez, 1998) in cells where it is endogenously expressed. Interestingly, recombinant expression of PTMA in *S. cerevisiae* is toxic, and this toxicity is dependent on the presence of a NLS in the C terminus of PTMA that facilitates its translocation into the yeast cell nucleus (Pavlov et al., 1995). Thus, PTMA may induce filamentation in *C. albicans* by engaging with a receptor on the fungal cell surface, by acting on an intracellular target, possibly within the nucleus, or by other as yet unknown mechanisms.

In addition to these key questions, what might be the consequences of the PTMA activity we have uncovered in the broader context of infection? *C. albicans* filamentation within macrophages has opposing implications for host and pathogen, where filamentation promotes activation of macrophage inflammatory cell death and fungal escape (O'Meara et al., 2015). Although immune cell death is a seemingly unfavorable outcome for the host, it releases pro-inflammatory cytokines that promote the recruitment of neutrophils, which are important effectors of fungal clearance (Netea et al., 2015; O'Meara et al., 2018). Thus, perhaps *C. albicans* filamentation within the macrophage phagosome indirectly favors host survival, and PTMA, along with physical factors such as nutrient deprivation (Lorenz et al., 2004), alkaline pH (Vylkova and Lorenz, 2014, 2017), and oxidative stress (Shi et al., 2007), serve to stimulate *C. albicans* filamentation in the phagosome as a strategy of self-sacrifice that promotes neutrophil recruitment and drives protective T cell responses (Richardson and Moyes, 2015). Our discovery of PTMA as a host factor that stimulates *C. albicans* filamentation potentially at the expense of phagocyte survival opens an interesting area of investigation into the molecular underpinnings of this organism's complex host-pathogen relationship.

STAR★METHODS

KEY RESOURCES TABLE

REAGENT or RESOURCE	SOURCE	IDENTIFIER
Antibodies		
N-terminal anti-PTMA antiserum	Abcam	Cat#ab14332; RRID:AB_301112
Non-immune rabbit serum	Abcam	Cat#ab166640
C-terminal anti-PTMA antibody	Abcam	Cat#ab200672

REAGENT or RESOURCE	SOURCE	IDENTIFIER
Polyclonal rabbit IgG control	Abcam	Cat#ab37415; RRID:AB_2631996
Chemicals, peptides, and recombinant proteins		
Rat PTMA	Abcam	Cat#ab226237
Deposited data		
Liquid-chromatography mass spectrometry of J774A.1 cell lysate	This paper; MassIVE repository	Tables S1 and S2; https://massive.ucsd.edu/ProteoSAFe/static/massive.jsp ; MSV000087532
Experimental models: Cell lines		
Mouse: J774A.1 cell line	ATCC	Cat#TIB-67; RRID:CVCL_0358
Mouse: RAW264.7 cell line	ATCC	Cat#TIB-71; RRID:CVCL_0493
Human: U937 cell line	ATCC	Cat#CRL-3253; RRID:CVCL_2Z95
Experimental models: Organisms/Strains		
<i>Candida albicans</i> : Strain background: HWP1p-GFP	Staab et al., 2003	N/A
<i>Candida albicans</i> : Strain background: SN95	Noble and Johnson, 2005	N/A
Software and algorithms		
iProphet	Shteynberg et al., 2011	http://tools.proteomecenter.org/software.php

RESOURCE AVAILABILITY

Lead contact—Further information and requests for resources and reagents should be directed to and will be fulfilled by the lead contact, Leah Cowen (leah.cowen@utoronto.ca).

Materials availability—This study did not generate any new unique reagents.

Data and code availability—The mass spectrometry dataset generated during this study is available at the MassIVE repository (<https://massive.ucsd.edu/ProteoSAFe/static/massive.jsp>) via the accession number MSV000087532. The ProteomeXchange accession is PXD026320.

This paper does not report original code.

Any additional information requested to reanalyze the data reported in this paper is available from the lead contact upon request.

EXPERIMENTAL MODEL AND SUBJECT DETAILS

***C. albicans* growth conditions**—*C. albicans* strains were grown under standard laboratory conditions at 30°C in yeast extract-peptone-dextrose (YPD) medium (1% yeast extract, 2% peptone, and 2% D-glucose). Strain archives were maintained in 25% glycerol in YPD medium at –80°C.

Culture of mammalian cell lines—J774A.1, RAW 264.7, and U937 cells were maintained in RPMI medium supplemented with 10% heat-inactivated fetal bovine serum (HI-FBS, GIBCO) at 37°C in the presence of 5.5% CO₂.

Preparation of bone marrow-derived macrophages—Bone marrow-derived macrophages (BMDMs) were generated by culturing bone marrow cells isolated from the femur and tibia of 6- to 8-week-old healthy female C57BL/6J mice (The Jackson Laboratory, JAX_000664). For differentiation, 5×10^6 cells were seeded into a 10 cm² Petri dish (VWR) in RPMI medium supplemented with 10% HI-FBS, 15% L929 fibroblast-conditioned medium as a source of macrophage colony stimulating factor, 100 U/L penicillin-streptomycin (GIBCO), and 2 mM L-glutamine (GIBCO) and incubated for seven days at 37 °C and 5.5% CO₂. Adherent cells were detached by incubating dishes in 10 mL ice-cold phosphate-buffered saline (PBS, Sigma) for 10 minutes at 4°C then gently pipetting the PBS across the dish.

METHOD DETAILS

Macrophage infection with *C. albicans*—J774A.1 cells or BMDMs were diluted to 1×10^5 cells/mL and 4×10^5 cells/mL, respectively in RPMI medium supplemented with 3% HI-FBS. Cell suspension (100 µL/well) was added to flat-bottom 96-well microtiter plates (Sarstedt) and incubated for 18 h at 37°C under 5.5% CO₂. The next day, an overnight culture of *C. albicans* strain *HWPIp*-GFP was diluted to 1×10^5 cells/mL in RPMI medium supplemented with 3% HI-FBS and fungal suspension (100 µL/well) was added to the wells of plates previously seeded with J774A.1 cells or BMDMs. Multiplicity of infection was optimized to enable visualization of a single engulfed fungal cell per immune cell. Co-cultures were incubated for 3 h at 37°C under 5.5% CO₂ at which time images were obtained using an AxioVision inverted microscope (Carl Zeiss) using phase contrast optics and white light illumination or an X-cite series 120 light source for fluorescence excitation.

Lysate preparation—J774A.1 cells, RAW 264.7 cells, U937 cells, and BMDMs were collected, washed twice with PBS, and concentrated to 4×10^7 cells/mL (cell lines) or 8×10^7 cells/mL (primary cells) in hypotonic buffer (10 mM Tris-HCl pH 7.5, 10 mM NaCl). To lyse cells, suspensions were subjected to three rapid freeze-thaw cycles using liquid nitrogen and a 30°C water bath. To verify lysis, suspensions were diluted 1:1 into Trypan Blue (GIBCO) and examined by light microscopy. Debris was pelleted by centrifugation at 13,200 rpm for 5 min at 4°C and clarified supernatants were incubated with phenylmethylsulfonyl fluoride (PMSF, 100 µM, BioShop) for 30 min on ice. Prior to proteinase or phosphatase treatment, clarified lysates were incubated for an additional 30 min at room temperature to ensure PMSF inactivation. Protein concentration was measured using a bicinchoninic acid protein assay (Pierce). Clarified lysates were aliquoted and stored at –80°C until further use.

Filamentation assay—Lysates were diluted into RPMI medium modified for growth of fungi (RPMI-based fungal medium: 10.4 g/L RPMI 1640 powder (Thermo Fisher Scientific), 3.5% morpholinepropanesulfonic acid (BioShop), 2% D-glucose (BioShop), 5 mg/mL histidine (Sigma), pH 7) to achieve the desired protein concentration. Cultures of

C. albicans were grown overnight in YPD medium at 30°C under static conditions, then diluted to an OD₆₀₀ of 0.085. Cells were then further diluted 1:20 into diluted lysates supplemented with 100 U/L penicillin-streptomycin in a flat-bottom 96-well microtiter plate (100 µL/well). Plates were incubated at 30°C for 6 h under static conditions then medium was replaced with PBS (100 µL/well) before imaging using the IncuCyte® S3 Live-Cell Analysis System (Sartorius). A growth temperature of 30°C was selected given that RPMI induces filamentation at 37°C in the absence of lysate, and an end-point of 6 hours was chosen to facilitate processing of filaments by flow cytometry as described below. To determine if incubation of *C. albicans* with 10% serum for 6 h at 30°C is sufficient to induce filamentation, filamentation assays were performed as described above with RPMI-based fungal medium supplemented with 10% HI-FBS.

Proteinase and phosphatase treatment—J774A.1 lysate (200 µg/mL) was incubated with proteinase K (100 µg/mL, Thermo Fisher #EO0491) or NEBuffer3 (1x, NEB #B7003) and heat-labile calf intestinal alkaline phosphatase (CIP, 280 U/mL, NEB #M0525) for 1 h at 37°C. Treated lysates were subsequently analyzed in filamentation assays as described above. To determine if proteinase K or CIP treatment alter *C. albicans* filamentation induced by elevated temperature, RPMI-based fungal medium was incubated with proteinase K or NEBuffer3 and CIP as described above. Cultures of *C. albicans* were grown overnight in YPD medium at 30°C under static conditions, then diluted to an OD₆₀₀ of 0.085. Cultures were further diluted 1:20 into RPMI with 100 U/L penicillin-streptomycin in a flat-bottom 96-well microtiter plate (100 µL/well). Plates were incubated at 42°C for 4.5 h under static conditions then medium was replaced with PBS (100 µL/well) before imaging using the IncuCyte® S3 Live-Cell Analysis System. Conditions were confirmed to not significantly impact CIP activity (data not shown).

Liquid-chromatography mass spectrometry—J774A.1 lysate was filtered through a 3 kDa MWCO modified polyethersulfone filter (Pall Corporation) then acidified with formic acid and fractionated using solid phase extraction columns that were prepared in-house by packing 10 cm of 5 µm C18 (Reprosil, Dr. Maische) into a 200 µm inner diameter (ID) tube that was fitted with polymerized Kasil solution. Sample (120 µg) and gradient solutions were added to the column using a gas pressurized column packing vessel, and eluting fractions were collected manually. Step gradients with increasing concentrations of acetonitrile were used to separate and elute peptides at 5%, 15%, 20%, 25%, 35%, 45%, 55%, and 65%. After evaporation of solvents, each fraction was re-dissolved in RPMI-based fungal medium and assayed for ability to induce *C. albicans* filamentation as described below. The same fractions were also analyzed for their peptide content by liquid-chromatography mass spectrometry (LCMS). Fractions analyzed by LCMS were first evaporated using a speed-vac to remove acetonitrile and then resuspended in 5% formic acid. Analysis was done using a Thermo Fusion Lumos instrument and an Eksigent 425 nanoLC with an in-house prepared 15 cm × 75 µm ID packed emitter column containing reverse phase C18 (3 µm, Reprosil, Dr. Maische). Acquisition was performed using a top 20 data dependent acquisition (DDA) method and a 90-min separation gradient (2%–35%) at 200 nL/min. DDA method included a high resolution MS1 scan, 20 high resolution higher-energy collision dissociation cell MS2 scans and a 15 s dynamic exclusion time.

Data analysis was performed with Mascot and Comet search algorithms, searching against a mouse database (RefSeq) and with parameters that included no-enzyme specificity, +/- 10 ppm parent mass and ± 0.05 Da fragment ion mass tolerances. Variable modifications included Met-oxidation. Search results were combined using iProphet (Shteynberg et al., 2011) and results were filtered at 0.95 probability.

Bioactivity analysis of eluted fractions—Cultures of *C. albicans* were grown overnight in YPD medium at 30°C under static conditions, then diluted to an OD₆₀₀ of 0.085. Cultures were further diluted 1:20 into reconstituted lysate fractions in a flat-bottom 384-well microtiter plate (20 μ L/well; Sarstedt). Plates were incubated at 30°C for 6 h under static conditions. Cells were imaged using differential interference contrast microscopy with a Zeiss Axio Imager.MI microscope (Carl Zeiss).

PTMA sufficiency assay—His-tagged rat PTMA purified from *S. cerevisiae* (10 μ g/mL, Abcam 226237) or glycerol (1.25%, BioShop) was added to the indicated concentration of J774A.1 lysate and subsequently analyzed in filamentation assays as described above. To confirm its purity and integrity, His-tagged rat PTMA purified from *S. cerevisiae* (1 μ g) was boiled in 1x Laemmli buffer for 5 minutes before fractionation on a 15% SDS-PAGE gel and visualization by Coomassie blue staining.

PTMA immunoneutralization assay—Aliquots of J774A.1 or BMDM lysate were incubated overnight at 4°C following addition of N-terminal anti-PTMA antiserum (10 μ g/mL, Abcam 14332), an equivalent volume of non-immune rabbit serum (Abcam 166640), C-terminal anti-PTMA antibody (20 μ g/mL, Abcam 200672), or polyclonal rabbit IgG control (20 μ g/mL, Abcam 37415). J774A.1 lysate was used at 300 μ g/mL for incubation with the N-terminal anti-PTMA antiserum or non-immune rabbit serum. For incubation with either the C-terminal anti-PTMA antibody or polyclonal rabbit IgG control, J774A.1 and BMDM lysates were used at 200 μ g/mL. After overnight incubation, lysates were analyzed for filament-inducing activity as described above. To determine if antibody treatment affects *C. albicans* filamentation induced by elevated temperature, RPMI-based fungal medium was incubated with each antibody preparation in isolation at the concentrations described above for 1 h at 4°C. Cultures of *C. albicans* were grown overnight in YPD medium at 30°C under static conditions, then diluted to an OD₆₀₀ of 0.085. Cells were further diluted 1:20 into RPMI with 100 U/L penicillin-streptomycin in a flat-bottom 96-well microtiter plate (100 μ L/well). Plates were incubated at 42°C for 4.5 h under static conditions then medium was replaced with PBS (100 μ L/well) before imaging using the IncuCyte® S3 Live-Cell Analysis System.

Flow cytometry—Cultures of *C. albicans* strain *HWPIp*-GFP were analyzed using a CytoFlex S flow cytometer (Beckman Coulter) to quantify GFP fluorescence. For these experiments, cells were treated as described above for IncuCyte® S3 Live-Cell imaging then resuspended by agitation with a plastic pinning comb and the entire volume of each well was transferred to a flat-bottom 96-well microtiter plate (Beckman Coulter). For each sample, ~5,000 events were captured in the P1 analysis gate, which discarded particulates and cellular debris. The percentage of GFP-positive events (%GFP+) in the FL1 channel was

quantified based on the number of gated events with a relative fluorescence intensity within a GFP+ boundary. The GFP+ boundary was defined as a region that included less than 3% of all gated events observed for non-induced control cultures.

QUANTIFICATION AND STATISTICAL ANALYSIS

Statistical significance of triplicate measurements was determined using an unpaired two-tailed t test in GraphPad Prism, version 9. Values of $p < 0.05$ were considered significant. Data are shown as the mean \pm standard deviation (SD). n represents the number of times an experiment was run with independent overnight cultures of *C. albicans*. Statistical details for each experiment can be found in the corresponding figure legend.

Supplementary Material

Refer to Web version on PubMed Central for supplementary material.

ACKNOWLEDGMENTS

We thank Cynthia Guo and Scott-Gray Owen for providing guidance and facilities and Alex Jaeger for providing constructs and advice for constructing PTMA knockdown macrophage cell lines. We thank Isobel Reckers, Jacqueline Watt, and Jun Liu for generously providing mouse bone marrow cells and L929 fibroblast-conditioned medium. Additionally, we thank all members of the Cowen laboratory for their instrumental support and helpful discussions. N.T.C. is supported by a Canadian Institutes for Health Research (CIHR) Canada Graduate Scholarships-Master's award. L.E.C. is supported by CIHR Foundation grant FDN-154288 and NIH grant R01AI127375, is a Canada Research Chair (Tier 1) in Microbial Genomics & Infectious Disease, and is Co-Director of the CIFAR Fungal Kingdom: Threats & Opportunities program. Proteomics work was performed at the Network Biology Collaborative Centre at the Lunenfeld-Tanenbaum Research Institute, a facility supported by Canada Foundation for Innovation funding, by the Government of Ontario, and by Genome Canada and Ontario Genomics (OGI-139). A.C.G. is a Canada Research Chair (Tier 1) in Functional Proteomics. The graphical abstract was created with BioRender.com.

REFERENCES

- Bain JM, Louw J, Lewis LE, Okai B, Walls CA, Ballou ER, Walker LA, Reid D, Munro CA, Brown AJP, et al. (2014). *Candida albicans* hypha formation and mannan masking of β -glucan inhibit macrophage phagosome maturation. *MBio* 5, e01874. [PubMed: 25467440]
- Bain JM, Alonso MF, Childers DS, Walls CA, Mackenzie K, Pradhan A, Lewis LE, Louw J, Avelar GM, Larcombe DE, et al. (2021). Immune cells fold and damage fungal hyphae. *Proc. Natl. Acad. Sci. USA* 118, e2020484118. [PubMed: 33876755]
- Baxevanis CN, Frillingos S, Seferiadis K, Reclus GJ, Arsenis P, Katsiyannis A, Anastasopoulos E, Tsolas O, and Papamichail M (1990). Enhancement of human T lymphocyte function by prothymosin α : increased production of interleukin-2 and expression of interleukin-2 receptors in normal human peripheral blood T lymphocytes. *Immunopharmacol. Immunotoxicol.* 12, 595–617. [PubMed: 2092041]
- Baxevanis CN, Thanos D, Reclus GJ, Anastasopoulos E, Tsokos GC, Papamatheakis J, and Papamichail M (1992). Prothymosin alpha enhances human and murine MHC class II surface antigen expression and messenger RNA accumulation. *J. Immunol.* 148, 1979–1984. [PubMed: 1545115]
- Bistoni F, Marconi P, Frati L, Bonmassar E, and Garaci E (1982). Increase of mouse resistance to *Candida albicans* infection by thymosin α 1. *Infect. Immun.* 36, 609–614. [PubMed: 7085074]
- Brown GD, Denning DW, Gow NAR, Levitz SM, Netea MG, and White TC (2012). Hidden killers: human fungal infections. *Sci. Transl. Med* 4, 165rv13.
- Cordero OJ, Sarandeses CS, López JL, and Nogueira M (1992). Prothymosin α enhances human natural killer cell cytotoxicity: role in mediating signals for NK activity. *Lymphokine Cytokine Res.* 11, 277–285. [PubMed: 1467368]

- Deutsch EW, Eng JK, Zhang H, King NL, Nesvizhskii AI, Lin B, Lee H, Yi EC, Ossola R, and Aebersold R (2005). Human plasma PeptideAtlas. *Proteomics* 5, 3497–3500. [PubMed: 16052627]
- Dickinson ME, Flenniken AM, Ji X, Teboul L, Wong MD, White JK, Meehan TF, Weninger WJ, Westerberg H, Adissu H, et al.; International Mouse Phenotyping Consortium; Jackson Laboratory; Infrastructure Nationale PHENOMIN, Institut Clinique de la Souris (ICS); Charles River Laboratories; MRC Harwell; Toronto Centre for Phenogenomics; Wellcome Trust Sanger Institute; RIKEN BioResource Center (2016). High-throughput discovery of novel developmental phenotypes. *Nature* 537, 508–514. [PubMed: 27626380]
- Erwig LP, and Gow NAR (2016). Interactions of fungal pathogens with phagocytes. *Nat. Rev. Microbiol.* 14, 163–176. [PubMed: 26853116]
- Evstafieva AG, Belov GA, Rubtsov YP, Kalkum M, Joseph B, Chichkova NV, Sukhacheva EA, Bogdanov AA, Pettersson RF, Agol VI, and Vartapetian AB (2003). Apoptosis-related fragmentation, translocation, and properties of human prothymosin alpha. *Exp. Cell Res.* 284, 211–223. [PubMed: 12651154]
- Fellmann C, Hoffmann T, Sridhar V, Hopfgartner B, Muhar M, Roth M, Lai DY, Barbosa IAM, Kwon JS, Guan Y, et al. (2013). An optimized microRNA backbone for effective single-copy RNAi. *Cell Rep.* 5, 1704–1713. [PubMed: 24332856]
- Gómez-Márquez J, and Rodríguez P (1998). Prothymosin α is a chromatinremodelling protein in mammalian cells. *Biochem. J.* 333, 1–3. [PubMed: 9639554]
- Heidecke H, Eckert K, Schulze-Forster K, and Maurer HR (1997). Prothymosin α 1 effects *in vitro* on chemotaxis, cytotoxicity and oxidative response of neutrophils from melanoma, colorectal and breast tumor patients. *Int. J. Immunopharmacol.* 19, 413–420. [PubMed: 9568546]
- Helmerhorst EJ, Breeuwer P, van't Hof W, Walgreen-Weterings E, Oomen LCJM, Veerman ECI, Amerongen AVN, and Abee T (1999). The cellular target of histatin 5 on *Candida albicans* is the energized mitochondrion. *J. Biol. Chem.* 274, 7286–7291. [PubMed: 10066791]
- Jiang X, Kim HE, Shu H, Zhao Y, Zhang H, Kofron J, Donnelly J, Burns D, Ng SC, Rosenberg S, and Wang X (2003). Distinctive roles of PHAP proteins and prothymosin- α in a death regulatory pathway. *Science* 299, 223–226. [PubMed: 12522243]
- Karetsov Z, Kretsovali A, Murphy C, Tsolas O, and Papamarcaki T (2002). Prothymosin α interacts with the CREB-binding protein and potentiates transcription. *EMBO Rep.* 3, 361–366. [PubMed: 11897665]
- Kijogi CM, Khayeka-Wandabwa C, Sasaki K, Tanaka Y, Kurosu H, Matsunaga H, and Ueda H (2016). Subcellular dissemination of prothymosin alpha at normal physiology: immunohistochemical vis-a-vis western blotting perspective. *BMC Physiol.* 16, 2. [PubMed: 26932824]
- Lo HJ, Köhler JR, DiDomenico B, Loebenberg D, Cacciapuoti A, and Fink GR (1997). Nonfilamentous *C. albicans* mutants are avirulent. *Cell* 90, 939–949. [PubMed: 9298905]
- Lorenz MC, Bender JA, and Fink GR (2004). Transcriptional response of *Candida albicans* upon internalization by macrophages. *Eukaryot. Cell* 3, 1076–1087. [PubMed: 15470236]
- Mandaliti W, Nepravishta R, Sinibaldi Vallebona P, Pica F, Garaci E, and Paci M (2016). Thymosin α 1 interacts with exposed phosphatidylserine in membrane models and in cells and uses serum albumin as a carrier. *Biochemistry* 55, 1462–1472. [PubMed: 26909491]
- Matejuk A, Leng Q, Begum MD, Woodle MC, Scaria P, Chou ST, and Mixson AJ (2010). Peptide-based antifungal therapies against emerging infections. *Drugs Future* 35, 197–217. [PubMed: 20495663]
- Matsunaga H, and Ueda H (2010). Stress-induced non-vesicular release of prothymosin- α initiated by an interaction with S100A13, and its blockade by caspase-3 cleavage. *Cell Death Differ.* 17, 1760–1772. [PubMed: 20467443]
- Murad AMA, Leng P, Straffon M, Wishart J, Macaskill S, MacCallum D, Schnell N, Talibi D, Marechal D, Tekaiia F, et al. (2001). *NRG1* represses yeast-hypha morphogenesis and hypha-specific gene expression in *Candida albicans*. *EMBO J.* 20, 4742–4752. [PubMed: 11532938]
- Nepravishta R, Mandaliti W, Eliseo T, Sinibaldi Vallebona P, Pica F, Garaci E, and Paci M (2015). Thymosin α 1 inserts N terminus into model membranes assuming a helical conformation. *Expert Opin. Biol. Ther.* 15 (Suppl 1), S71–S81. [PubMed: 25642593]

- Netea MG, Joosten LAB, van der Meer JWM, Kullberg BJ, and van de Veerdonk FL (2015). Immune defence against *Candida* fungal infections. *Nat. Rev. Immunol.* 15, 630–642. [PubMed: 26388329]
- Noble SM, and Johnson AD (2005). Strains and strategies for large-scale gene deletion studies of the diploid human fungal pathogen *Candida albicans*. *Eukaryot. Cell* 4, 298–309. [PubMed: 15701792]
- Noble SM, French S, Kohn LA, Chen V, and Johnson AD (2010). Systematic screens of a *Candida albicans* homozygous deletion library decouple morphogenetic switching and pathogenicity. *Nat. Genet.* 42, 590–598. [PubMed: 20543849]
- O’Meara TR, Veri AO, Ketela T, Jiang B, Roemer T, and Cowen LE (2015). Global analysis of fungal morphology exposes mechanisms of host cell escape. *Nat. Commun.* 6, 6741. [PubMed: 25824284]
- O’Meara TR, Duah K, Guo CX, Maxson ME, Gaudet RG, Koselny K, Wellington M, Powers ME, MacAlpine J, O’Meara MJ, et al. (2018). High-throughput screening identifies genes required for *Candida albicans* induction of macrophage pyroptosis. *MBio* 9, e01581–18. [PubMed: 30131363]
- Pavlov N, Evstafieva A, Rubtsov Y, and Vartapetian A (1995). Human prothymosin α inhibits division of yeast *Saccharomyces cerevisiae* cells, while its mutant lacking nuclear localization signal does not. *FEBS Lett.* 366, 43–45. [PubMed: 7789513]
- Polvi EJ, Li X, O’Meara TR, Leach MD, and Cowen LE (2015). Opportunistic yeast pathogens: reservoirs, virulence mechanisms, and therapeutic strategies. *Cell. Mol. Life Sci.* 72, 2261–2287. [PubMed: 25700837]
- Richardson JP, and Moyes DL (2015). Adaptive immune responses to *Candida albicans* infection. *Virulence* 6, 327–337. [PubMed: 25607781]
- Rivas-Santiago B, Hernandez-Pando R, Carranza C, Juarez E, Contreras JL, Aguilar-Leon D, Torres M, and Sada E (2008). Expression of cathelicidin LL-37 during *Mycobacterium tuberculosis* infection in human alveolar macrophages, monocytes, neutrophils, and epithelial cells. *Infect. Immun.* 76, 935–941. [PubMed: 18160480]
- Roh JS, and Sohn DH (2018). Damage-associated molecular patterns in inflammatory diseases. *Immune Netw.* 18, e27. [PubMed: 30181915]
- Romani L, Bistoni F, Gaziano R, Bozza S, Montagnoli C, Perruccio K, Pitzurra L, Bellocchio S, Velardi A, Rasi G, et al. (2004). Thymosin α 1 activates dendritic cells for antifungal Th1 resistance through toll-like receptor signaling. *Blood* 103, 4232–4239. [PubMed: 14982877]
- Samara P, Ioannou K, and Tsitsilonis OE (2016). Prothymosin alpha and immune responses. Are we close to potential clinical applications? *Vitam Horm* 102, 179–207. [PubMed: 27450735]
- Samaras P, Schmidt T, Frejno M, Gessulat S, Reinecke M, Jarzab A, Zecha J, Mergner J, Giansanti P, Ehrlich HC, et al. (2020). ProteomicsDB: a multi-omics and multi-organism resource for life science research. *Nucleic Acids Res.* 48 (D1), D1153–D1163. [PubMed: 31665479]
- Saville SP, Lazzell AL, Monteagudo C, and Lopez-Ribot JL (2003). Engineered control of cell morphology *in vivo* reveals distinct roles for yeast and filamentous forms of *Candida albicans* during infection. *Eukaryot. Cell* 2, 1053–1060. [PubMed: 14555488]
- Schmidt T, Samaras P, Frejno M, Gessulat S, Barnert M, Kienegger H, Krcmar H, Schlegl J, Ehrlich HC, Aiche S, et al. (2018). ProteomicsDB. *Nucleic Acids Res.* 46 (D1), D1271–D1281. [PubMed: 29106664]
- Shapiro RS, and Cowen LE (2012). Uncovering cellular circuitry controlling temperature-dependent fungal morphogenesis. *Virulence* 3, 400–404. [PubMed: 22722338]
- Shapiro RS, Robbins N, and Cowen LE (2011). Regulatory circuitry governing fungal development, drug resistance, and disease. *Microbiol. Mol. Biol. Rev.* 75, 213–267. [PubMed: 21646428]
- Shi QM, Wang YM, Zheng XD, Lee RTH, and Wang Y (2007). Critical role of DNA checkpoints in mediating genotoxic-stress-induced filamentous growth in *Candida albicans*. *Mol. Biol. Cell* 18, 815–826. [PubMed: 17182857]
- Shteynberg D, Deutsch EW, Lam H, Eng JK, Sun Z, Tasman N, Mendoza L, Moritz RL, Aebersold R, and Nesvizhskii AI (2011). iProphet: Multi-level integrative analysis of shotgun proteomic data improves peptide and protein identification rates and error estimates. *Mol. Cell. Proteomics* 10, M111.007690.

- Staab JF, Bahn YS, and Sundstrom P (2003). Integrative, multifunctional plasmids for hypha-specific or constitutive expression of green fluorescent protein in *Candida albicans*. *Microbiology (Reading)* 149, 2977–2986. [PubMed: 14523129]
- Sudbery PE (2011). Growth of *Candida albicans hyphae*. *Nat. Rev. Microbiol.* 9, 737–748. [PubMed: 21844880]
- Tsherniak A, Vazquez F, Montgomery PG, Weir BA, Kryukov G, Cowley GS, Gill S, Harrington WF, Pantel S, Krill-Burger JM, et al. (2017). Defining a cancer dependency map. *Cell* 170, 564–576.e16. [PubMed: 28753430]
- Vylkova S, and Lorenz MC (2014). Modulation of phagosomal pH by *Candida albicans* promotes hyphal morphogenesis and requires Stp2p, a regulator of amino acid transport. *PLoS Pathog.* 10, e1003995. [PubMed: 24626429]
- Vylkova S, and Lorenz MC (2017). Phagosomal neutralization by the fungal pathogen *Candida albicans* induces macrophage pyroptosis. *Infect. Immun.* 85, e00832–16. [PubMed: 27872238]
- Wartenberg A, Linde J, Martin R, Schreiner M, Horn F, Jacobsen ID, Jenull S, Wolf T, Kuchler K, Guthke R, et al. (2014). Microevolution of *Candida albicans* in macrophages restores filamentation in a nonfilamentous mutant. *PLoS Genet.* 10, e1004824. [PubMed: 25474009]

Highlights

- Lysates derived from macrophages robustly induce *C. albicans* filamentation
- Enzymatic treatment of lysate implicates a phosphoprotein in its activity
- Mass spectrometry identifies prothymosin alpha (PTMA) as a filament-inducing factor
- Immunoneutralization of PTMA blocks lysate induction of *C. albicans* filamentation

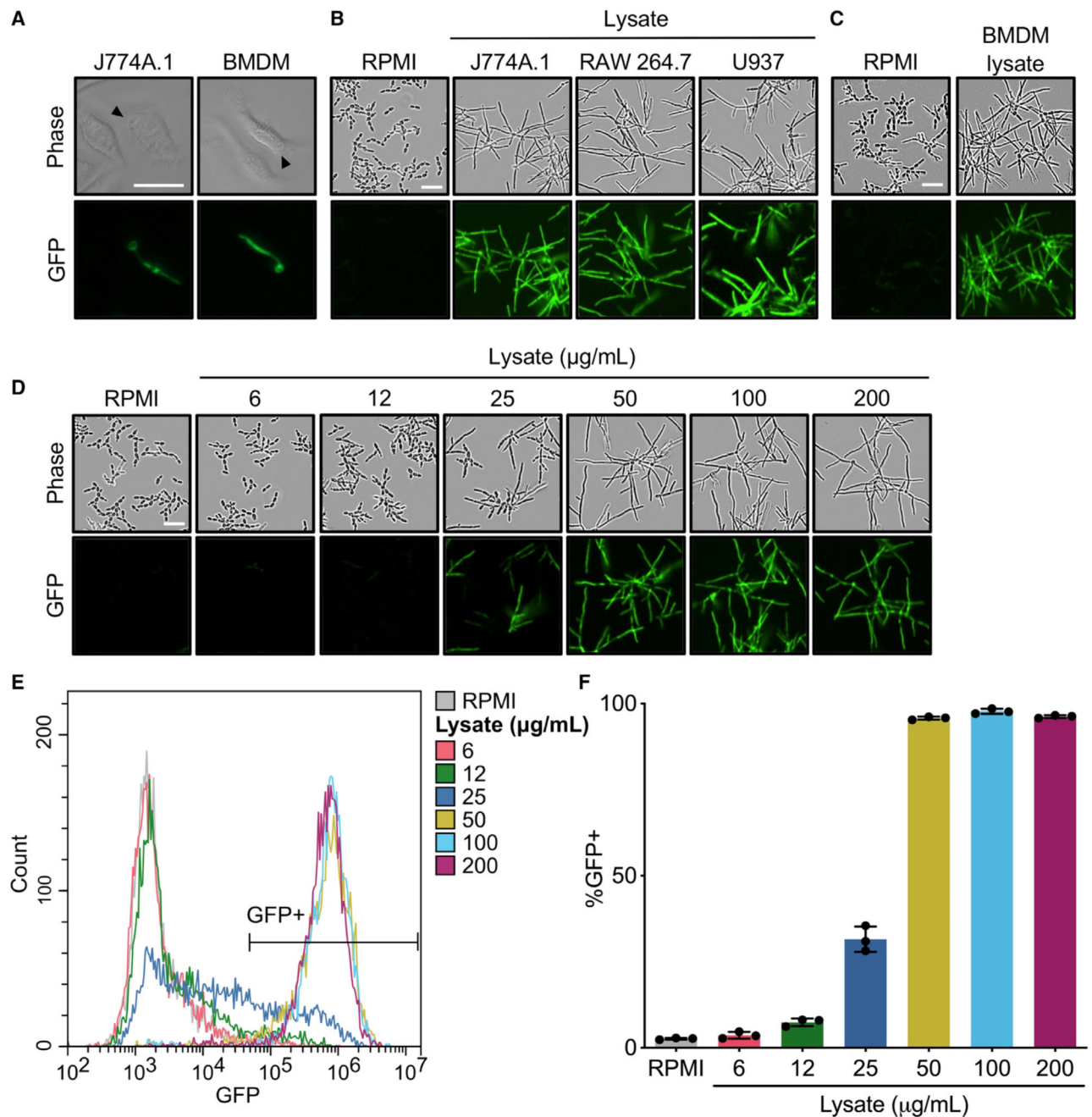


Figure 1. Lysates derived from macrophage-like cell lines and primary macrophages induce *C. albicans* filamentation

(A) Internalization by macrophage-like J774A.1 cells and murine bone marrow-derived macrophages (BMDMs) induces *C. albicans* filamentation. Cultures of J774A.1 cells or BMDMs were infected with a *C. albicans* strain expressing GFP from the hyphal-specific *HWP1* promoter (*HWP1p*-GFP). Representative images were acquired 3 h after infection at a multiplicity of 1:5 or 1:4 fungal to mouse cells for J774A.1 cells and BMDMs, respectively. Black arrowheads indicate ingested *C. albicans* mother cell from which a filament extends.

(B) Lysates from monocyte- and macrophage-like cell lines induce *C. albicans* filamentation. Representative images of the *HWP1p*-GFP strain incubated with J774A.1, RAW 264.7, or U937 lysates diluted in RPMI for 6 h at 30°C.

(C) Lysate derived from murine BMDMs induces *C. albicans* filamentation. Representative images of the *HWP1p*-GFP strain incubated with BMDM lysate diluted in RPMI for 6 h at 30°C.

(D–F) J774A.1 lysate induces *C. albicans* filamentation in a concentration-dependent manner. (D) Representative images of the *HWP1p*-GFP strain incubated with varying concentrations of J774A.1 lysate for 6 h at 30°C. (E) Analysis of *C. albicans* samples presented in (D) by flow cytometry. Histograms depict the distribution of relative green fluorescence intensity for ~5,000 gated events per sample. (F) Extent of lysate-induced filamentation in *C. albicans* populations exposed to the indicated concentrations of lysate as monitored by GFP expression. Each bar depicts the mean percent GFP⁺ (%GFP⁺) cells determined for technical triplicates. The %GFP⁺ cells are defined by the GFP⁺ region shown in (E). Error bars indicate SD for technical triplicates.

For the entire figure, data are representative of two biological replicates (n = 2). Scale bars: 25 μm. See also Figure S1.

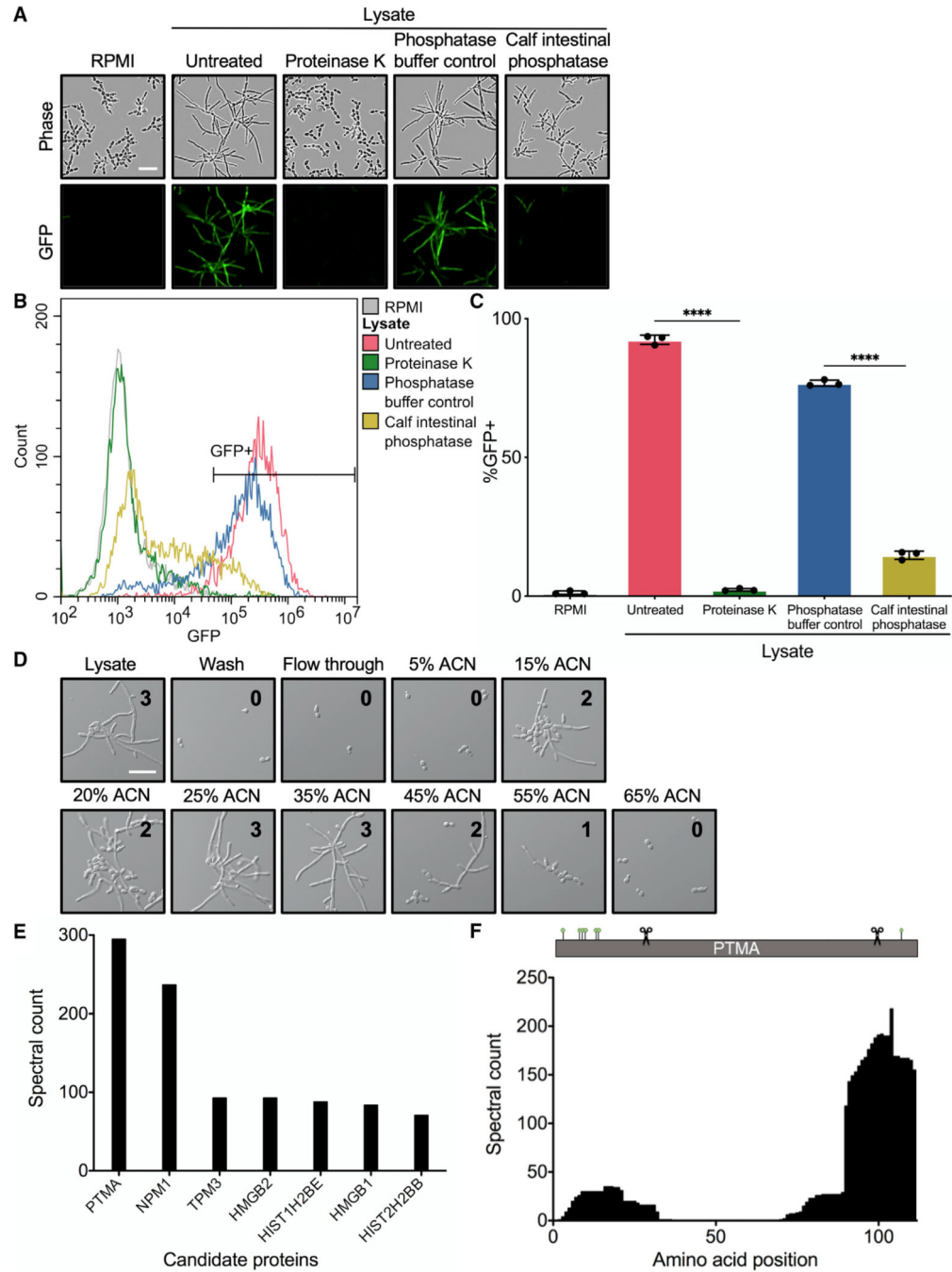


Figure 2. Bioactivity-guided fractionation of macrophage lysate coupled to mass spectrometry (MS) identifies candidate filament-inducing proteins

(A–C) A filament-inducing component in macrophage lysate is likely a phosphorylated protein. (A) Representative images of the *HWPIp*-GFP strain incubated for 6 h at 30°C with J774A.1 lysate that had been pre-treated with Proteinase K, phosphatase buffer alone as a control, or calf intestinal phosphatase. (B) Analysis of *C. albicans* cells in (A) by flow cytometry as described for Figure 1E. (C) Quantification of flow cytometry data in (B) as described for Figure 1F. Error bars indicate SD for technical triplicates, and statistical

significance was calculated using a two-sided unpaired t test. ****p = 0.0001. For (A)–(C), data are representative of two biological replicates (n = 2).

(D) Fractionation of macrophage lysate by reverse-phase liquid chromatography identifies robust filament-inducing activity in the fractions eluted with 25% and 35% acetonitrile (ACN). Representative images of *C. albicans* strain SN95 incubated with J774A.1 lysate fractions for 6 h at 30°C. Fractions were scored for their filament-inducing activity on a scale from 0 to 3, where 0 signifies yeast, 1 signifies short filaments or pseudohyphae, 2 signifies a mixed population of yeast and filaments, and 3 signifies predominantly filaments. Filamentation score for each fraction is indicated in the top right corner of the corresponding image.

(E) MS analysis of fractions identifies the greatest number of spectra corresponding to the immunomodulatory protein prothymosin alpha (PTMA) in the 35% ACN fraction. Spectral counts for seven proteins with the highest number of spectra in the fraction eluted with 35% ACN is shown. (F) Most spectra detected in the 35% ACN fraction for peptides mapped to PTMA mapped to its C terminus. Histogram depicting the number of peptides mapped to each amino acid residue of PTMA according to their position along the protein sequence from N to C terminus. Gray bar depicts PTMA sequence, green circles indicate phosphorylated residues, and scissors indicate sites of endogenous cleavage. For (D)–(F), data are representative of one biological replicate (n = 1). Scale bars: 25 μm. HIST1H2BE, histone cluster 1, H2be; HIST2H2BB, histone cluster 2, H2bb; HMGB1, high-mobility group box 1; HMGB2, high-mobility group box 2; NPM1, nucleophosmin 1; PTMA, prothymosin alpha; TPM3, tropomyosin alpha-3 chain. See also Tables S1 and S2 and Figures S1 and S2.

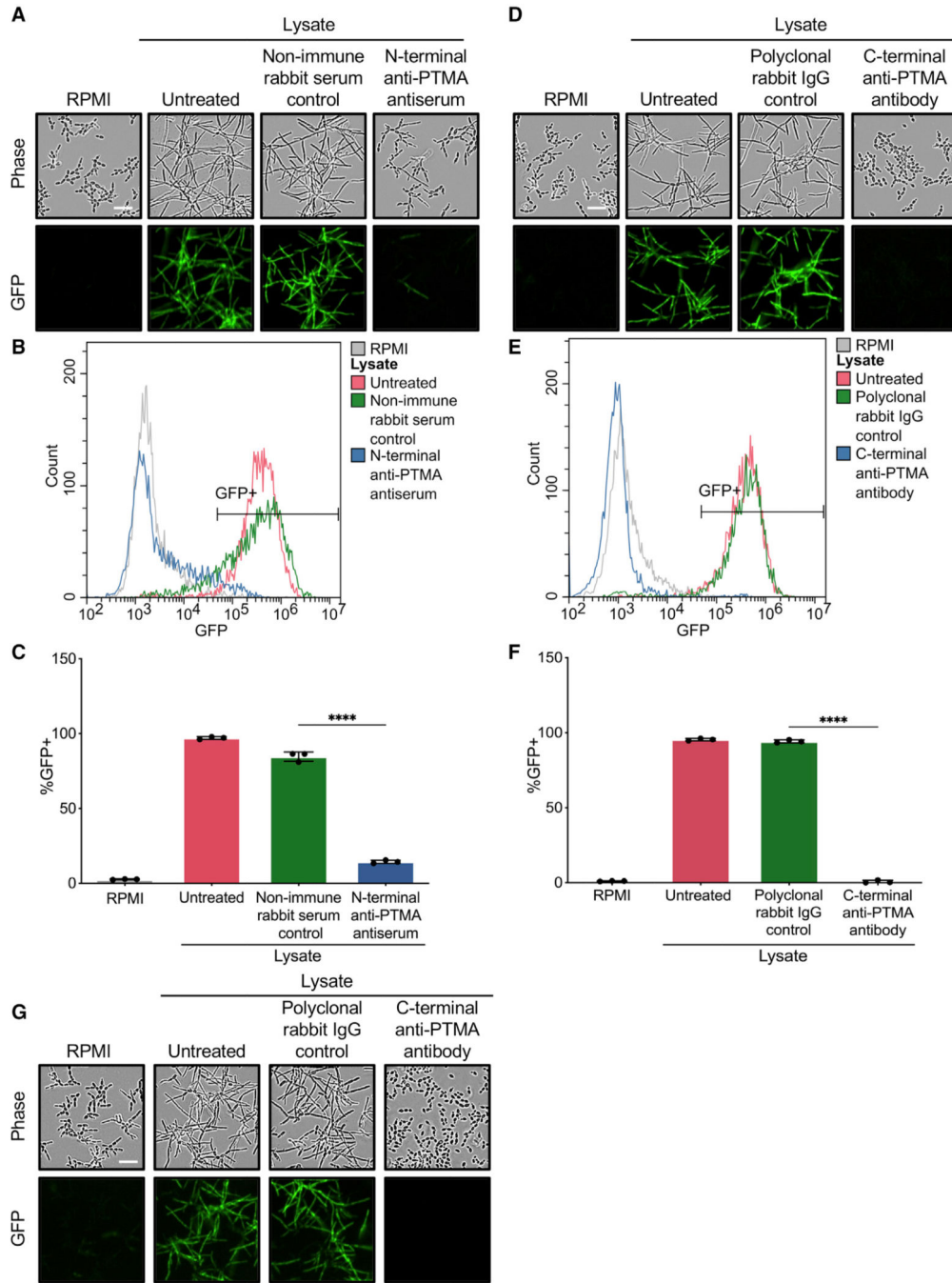


Figure 3. Immunoneutralization of PTMA reduces the filament-inducing activity of macrophage lysate

(A–C) Targeting of PTMA in macrophage lysate using an N-terminal anti-PTMA antiserum reduces the ability of lysate to induce filamentation. (A) Representative images of the *HWP1p*-GFP strain incubated with J774A.1 lysate for 6 h at 30°C. Lysate was pre-incubated overnight with an antiserum against the N terminus of PTMA or non-immune rabbit serum as control. (B) Analysis of *C. albicans* cells in (A) by flow cytometry as described for Figure 1E. (C) Quantification of flow cytometry data in (B) as described for Figure 1F.

(D–F) Targeting of PTMA in macrophage lysate using an affinity-purified antibody to a C-terminal epitope in PTMA abolishes the ability of lysate to induce filamentation. (D) Representative images of *C. albicans* strain *HWP1p*-GFP incubated with lysate for 6 h at 30°C. J774A.1 lysate was pre-incubated overnight with a C-terminal anti-PTMA antibody or polyclonal rabbit IgG as control. (E) Analysis of *C. albicans* cells in (D) by flow cytometry as described for Figure 1E. (F) Quantification of flow cytometry data in (E) as described for Figure 1F. For (C) and (F), error bars indicate SD for technical triplicates, and statistical significance was calculated using a two-sided unpaired t test. **** $p < 0.0001$. For (A)–(F), data are representative of three biologically independent experiments ($n = 3$).

(G) Immunoneutralization of PTMA abolishes the ability of BMDM lysate to induce *C. albicans* filamentation. Representative images of *C. albicans* strain *HWP1p*-GFP incubated with BMDM lysate for 6 h at 30°C. J774A.1 lysate was pre-incubated overnight with a C-terminal anti-PTMA antibody or polyclonal rabbit IgG as control. Data are representative of two biological replicates ($n = 2$).

Scale bars: 25 μm . See also Figures S1 and S3.